Journal of Macromolecular Science, Part A
Publication details, including instructions for authors and subscription information:
http://www.informaworld.com/smpp/title~content=t713597274

Polyimide-silica Hybrids: Structural and Morphological Investigations

Shaukat Saeed[a]; Muhammad Khalil[a]; Zahoor Ahmad[b]
[a] Department of Chemical and Materials Engineering, Pakistan Institute of Engineering and Applied Sciences (PIEAS), Islamabad, Pakistan [b] Department of Chemistry, Faculty of Science, Kuwait University, Safat, State of Kuwait

To cite this Article Saeed, Shaukat , Khalil, Muhammad and Ahmad, Zahoor(2009) 'Polyimide-silica Hybrids: Structural and Morphological Investigations', Journal of Macromolecular Science, Part A, 46: 2, 152 — 162

To link to this Article: DOI: 10.1080/10601320802594717

URL: http://dx.doi.org/10.1080/10601320802594717

Journal of Macromolecular Science®, Part A: Pure and Applied Chemistry (2009) **46**, 152–162
Copyright © Taylor & Francis Group, LLC
ISSN: 1060-1325 print / 1520-5738 online
DOI: 10.1080/10601320802594717

Polyimide-silica Hybrids: Structural and Morphological Investigations

SHAUKAT SAEED[1], MUHAMMAD KHALIL[1] and ZAHOOR AHMAD[2]*

[1]*Department of Chemical and Materials Engineering, Pakistan Institute of Engineering and Applied Sciences (PIEAS), Islamabad-45650, Pakistan*
[2]*Department of Chemistry, Faculty of Science, Kuwait University, Safat-13060, State of Kuwait*

Received June 2008 and accepted July 2008

Polyimide (PI) containing pendant hydroxyl functional groups have been employed for preparation of PI-silica hybrids through the sol-gel process. A stoichiometric amount of pyromellitic dianhydride (PMDA) was reacted with a mixture of oxydianiline (ODA) and 3,3′-diamino-4,4′-dihydroxybiphenyl (DAHP) in dimethylacetamide (DMAc) solvent to prepare the precursor poly(amic acid) (PAA) solution for the PI. Various proportions of tetraethoxysilane (TEOS) were mixed with PAA to prepare PI-silica hybrids through sol-gel process. The structure and morphology of these hybrids were investigated with field emission scanning electron microscopy (FE-SEM), transmission electron microscopy (TEM), optical surface profilometery, and Fourier transform infrared (FTIR) spectroscopy and compared with the one in which the matrix was prepared from PMDA and ODA with no pendant hydroxyl functionalities. Formation of silica lean and silica rich phases (SLP and SRP) as a result of formation of nano-sized silica clusters with diffused boundaries, dispersed in the matrix and their agglomerates, respectively, along with totally different morphology suggest a strong influence of hydroxyl groups in controlling the morphology of PI-silica hybrids. A model namely "*Retain and React*" has been introduced to explain observed structure.

Keywords: Polyimide, silica, hybrids, sol-gel, morphology

1 Introduction

Polyimides (PIs) are among the high performance polymers as they exhibit outstanding thermal stability, high mechanical strength, and good dielectric properties (1,2). Properties and performance of PIs can be improved by incorporating silicate component yielding a new material in the form of organic-inorganic hybrids. Sol-gel process has been used extensively in the past two decades to prepare PI-silica hybrids where silica particles were dispersed in the PI matrices (3–6). Such materials are reported to possess superior thermal stability, high refractive index, low coefficient of thermal expansion, and good mechanical properties. Improvement in properties of organic-inorganic hybrids is believed to be the outcome of physical/chemical interaction between organic and inorganic phases at the interface. A number of studies (7–12) have been conducted in past to improve interfacial interaction and hence to avoid or to at least minimize the phase separation between PI and silica components by incorporating different coupling agents. Surface modification of the inorganic particles is also considered to be a suitable method for tailoring sol-gel materials to make them compatible with the PI matrix through improved interfacial interaction (10–11).

Modification of the matrix itself in a way that leads toward creation of additional reactive sites for subsequent chemical interaction of the matrix with the inorganic network structure has also been proved to be an alternate to the particle's surface modification or addition of coupling agents. Modified PIs containing pendant hydroxyl groups along with some coupling agents have been prepared and used for the synthesis of PI-silica composites. Chen et al. (13) synthesized PI-silica hybrids with phenolic hydroxyl pendant groups using diamine monomer 4,4′-diamino-4″-hydroxytriphenylmethane. A coupling agent, 3-glycidyloxypropyl trimethoxysilane (GPTMOS), was also used to improve compatibility. Improvement in transparency, thermal and mechanical properties along with reduction in particle size, has been attributed to the presence of GPTMOS in the modified PI having hydroxyl groups.

Ahmad et al. (14, 15) and Huang et al. (16, 17) prepared PI-silica hybrids from pendant hydroxyl groups bearing PIs without using any coupling agent. The hydroxyl groups retarded gross phase separation through the formation of secondary bonds between PI and silica phase which resulted

---

*Address correspondence to: Zahoor Ahmad, Department of Chemistry, Faculty of Science, Kuwait University, Safat-13060, State of Kuwait. E-mail: zahoor-ahmad@live.com

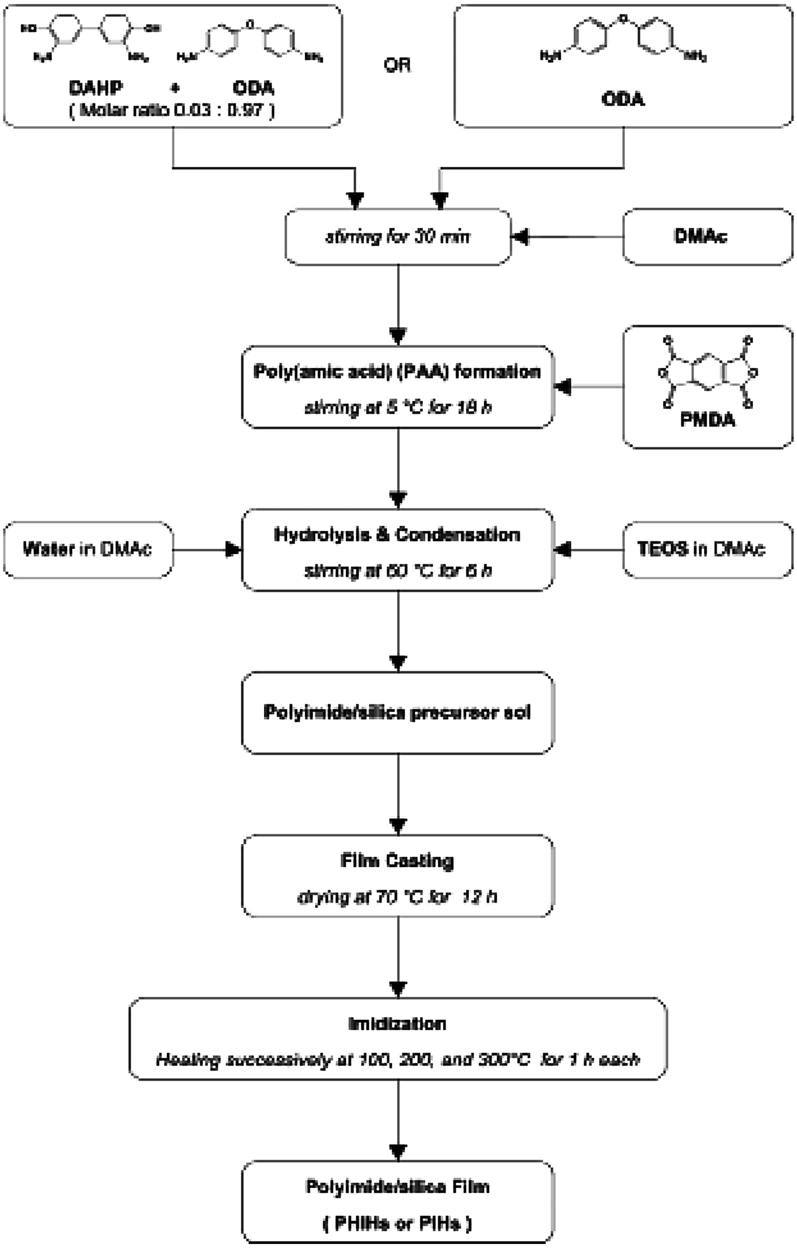

Fig. 1. Flow chart diagram for the synthesis of polyimide/silica hybrids (PHIHs and PIHs).

in the formation of nano-sized co-continuous domains as compared to the corresponding PI system having no hydroxyl groups. This also had a positive influence on the thermal and mechanical properties of the resulting hybrids.

Qin et al. (18) investigated phase separation process of the PI-silica hybrid films using scattering electron microscopy (SEM) and explained it in terms of interaction between carboxyl and hydroxyl groups. A double phase separation was reported in the preparation of the hybrid films. Evaporation of the solvent below 100°C caused a decrease in miscibility of TEOS in PAA and the first phase separation took place and yielded around 2 μm sized particles. The second phase separation from the matrix phase appeared, as PAA was imidized at elevated temperature, which destroyed the interaction between carboxyl group of PAA and hydroxyl group of TEOS, and a nano-scale SiO_2 particle phase formed. The formation mechanism of the double phase separation was explained by the "capture-release" model.

In the present work, the PI matrix with pendant hydroxyl groups was prepared by reacting a mixture of oxydianiline (ODA) and 3,3′-diamino-4,4′-dihydroxybiphenyl (DAHP) in dimethylacetamide (DMAc) with equimolar amount of pyromellitic dianhydride (PMDA). The addition of DAHP

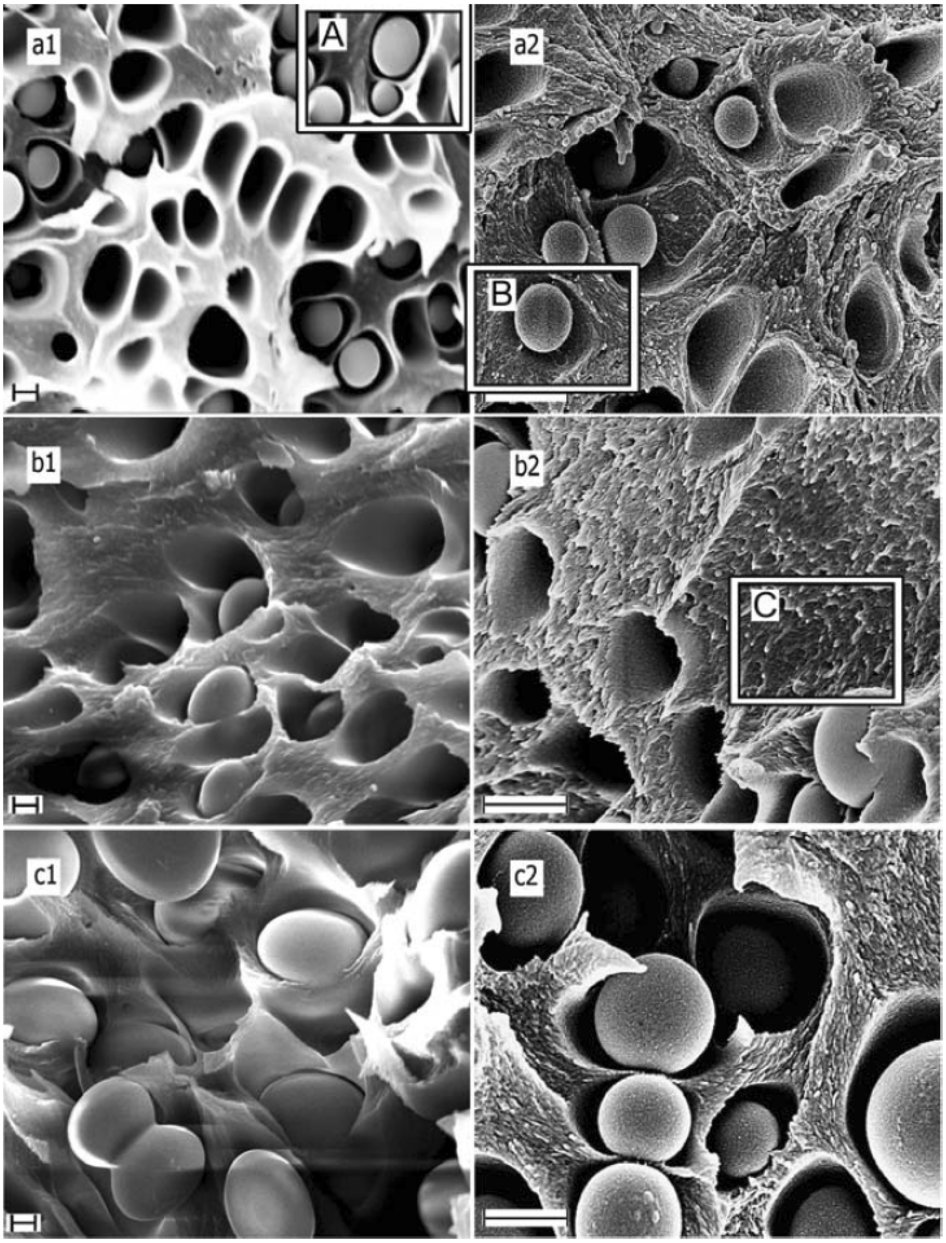

Fig. 2. FE-SEM micrographs each havine scale bar of 1 μm of (a1) PIH-10; (a2) PHIH-10; (b2) PHIH-20; (c1) PIH-30; (c2) PHIH-30.

ensures the inclusion of pendant hydroxyl groups in the matrix chains. Silica network was produced from TEOS through sol-gel process. The presence of hydroxyl groups, distributed on the matrix chain is expected to provide bonding sites for the *in situ* generated silica species thus modifying the morphology of the resulting hybrids. Effect of hydroxyl group bearing PI matrix on the morphology of the resulting PI-silica hybrids and on the size of silica particles was investigated using microscopic and spectroscopic techniques. Apparently two types of population of silica particles as reported by others (18, 19) were observed in this work. However, detailed morphological studies using SEM, TEM and profilometry revealed interesting information that could not be fully explained on the basis of Nandi's (2), Inoue's), and Qin's (18) proposed models. An effort has been made in the present work to explain the modification of network structure, creation of polymer-trapped nano-sized silica clusters and existence of covalent linkages between organic and inorganic phases in PI-silica systems. FTIR has also been utilized to correlate the observed morphological features with the structural details information from IR spectra.

2 Experimental

2.1 Materials

Pyromellitic dianhydride (PMDA; 99.2%; Aldrich), Dimethylacetamide (DMAc; 99.8%, anhydrous; Aldrich), 4,4'-Oxydianiline (ODA; 99.9%; Fluka), Tetraethoxysilane (TEOS; 97.5%; Acros), and 3,3′-Diamino-4,4′-dihydroxybiphenyl (DAHP; 98%; Tokyo Kasei Kogyo, Japan) were used as received.

2.2 Reaction Conditions

The two-step PI synthesis method shown in the flow sheet diagram (Fig. 1) was used. Keeping in view the tendency of DMAc to readily absorb moisture and high reactivity of PMDA with water, the polymerization reactions were carried out at low temperature (around 5°C) and under complete anhydrous conditions. The anhydrous inert conditions were achieved in an air-tight glove box by continuous forced circulation of nitrogen gas in a closed-loop over dried calcium chloride and directing it on a refrigerated plate fitted within the glove box where the reaction was conducted.

2.3 Preparation of PAA with Pendant Hydroxyl Groups

The PAA with pendant hydroxyl groups was prepared by the reaction of a mixture of ODA and DAHP taken, respectively in molar ratio 0.97:0.03 with a stoichiometric amount of PMDA in anhydrous DMAc. A 500 ml three-necked flask, fitted with a mechanical stirrer, was charged with 0.05 mols of diamines. The ODA 0.0485 mols (9.7194 g) and DAHP 0.0015 mols (0.3244 g) were taken and dissolved in 130 g of DMAc by stirring the solution for 30 min. A stoichiometric amount of PMDA, 0.05 mols (10.9940 g) was added at once to the vigorously stirred solution of amines that resulted in a highly viscous PAA solution. After 6 h of the polymerization reaction, 0.5% (0.0550 g) additional amount of PMDA was added that further increased PAA viscosity. In order to facilitate stirring the required amount of DMAc was added further to obtain 6 wt% (solid content) PAA solution. Polymerization reaction was performed for additional 12 h after which the reaction was assumed to be complete. The resulting PAA was used as stock solution and preserved at −20°C for subsequent use.

2.4 Preparation of PAA without Pendant Hydroxyl Groups

The PAA without pendant hydroxyl groups was synthesized by adopting a similar procedure as described above. A 0.05 mols (10.0200 g) of ODA was dissolved in 130 g of DMAc by stirring the solution for 30 min. A stoichiometric amount of PMDA, 0.05 moles (10.9940 g) was added at once to the vigorously stirred ODA solution. A sharp increase in the viscosity of PAA was observed after 15 min. Addition of 0.5% excess PMDA and DMAc was carried out after similar intervals as in above mentioned synthesis. Polymerization reaction was continued for 12 h and the resulting 6 wt% PAA was used as stock solution.

2.5 Preparation of Hybrid Films

The hybrid films were prepared by carrying out the*in situ* generation of silica structures in the PAA solutions through the sol-gel process. Various proportions of TEOS (as 20 wt % solution in DMAc) were added to the PAA solution to yield hybrids with different silica contents in the two matrices. A stoichiometric amount (TEOS:H_2O mol ratio 1:2) of water (as 10 wt% 0.1 M HCl solution in DMAc) was added to carry out hydrolysis and condensation reactions under acid catalyzed condition. The resulting mixtures were stirred for 6 h at 60°C. Hybrids with various silica contents ranging from 5–30 wt% were prepared and films were cast by solvent elution under inert atmosphere at 70°C for 12 h in the Teflon Petri dish. The films were further dried at 80°C for 6 h under vacuum. The imidization process was carried out by heating the films at 100, 200, and 300°C in sequence each for 1 h under nitrogen. The hybrids films thus prepared from the PI matrix without and with pendant hydroxyl groups matrices are named as PIH-x and PHIH-x respectively, where 'x' represents wt % of the silica used in the matrix. Table 1 shows the compositions of all samples of PIH-x

Table 1. Composition of PIH-x and PHIH-x hybrid Systems

Hybrid System	*Code*	*PI (wt%)*	*Silica (wt%)*	*ODA:DAHP (Molar Ratio)*	*TEOS:H_2O (Molar Ratio)*	*TEOS/OH (Molar Ratio)*
PIH-x	PIH-0	100	0	1:0	1:2	0
	PIH-10	90	10	1:0	1:2	0
	PIH-20	80	20	1:0	1:2	0
	PIH-30	70	30	1:0	1:2	0
PHIH-x	PHIH-0	100	0	0.97:0.03	1:2	0
	PHIH-10	90	10	0.97:0.03	1:2	10.9
	PHIH-20	80	20	0.97:0.03	1:2	24.6
	PHIH-30	70	30	0.97:0.03	1:2	42.9

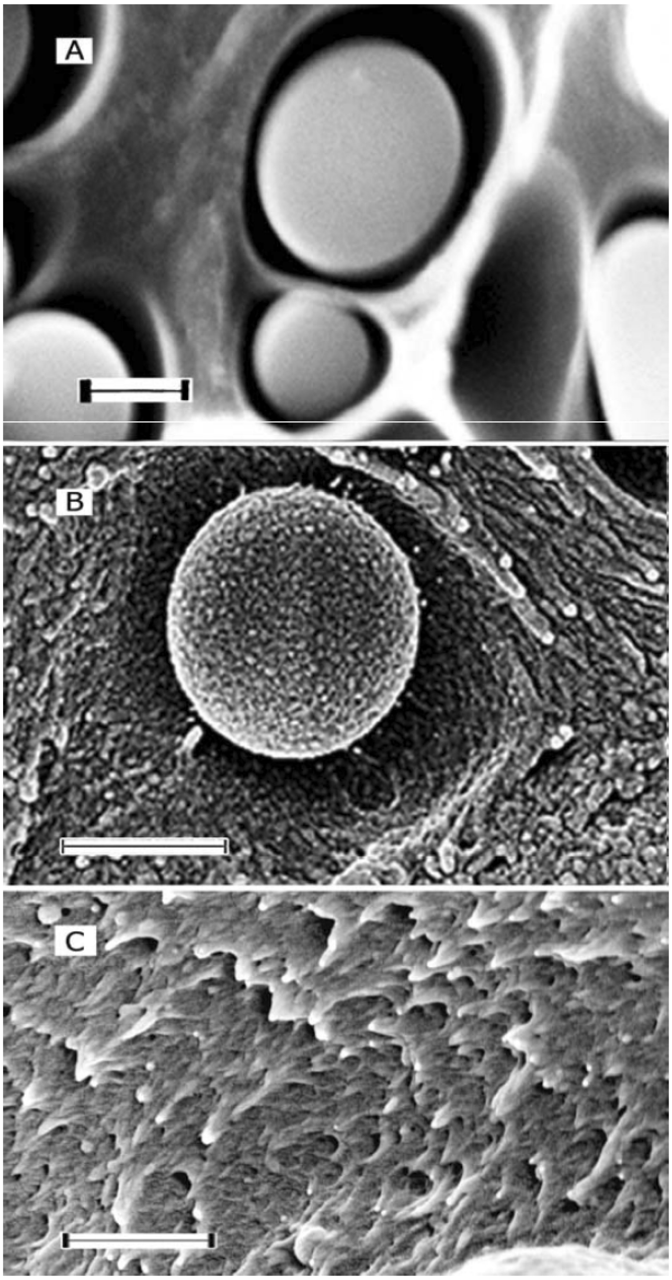

Fig. 3. High magnification FE-SEM micrographs of selected portion of: (A) PIH-10; (B) PHIH-10; (C) PHIH-20 Scale bar of (A) 1 μm; (B) 500 nm; (C) 500 nm.

and PHIH-x hybrid systems. The flow sheet diagram for the synthesis of the PAA and hybrids is given in the Figure 1.

2.6 Characterization of the Hybrid Films

The morphology of the hybrid films was studied using LEO 1550 Schottky field emission scanning electron microscope (FE-SEM). The samples were quenched in liquid nitrogen, and brittle fractured. These were vacuum dried at 0.2 mbar for 8 h at 100°C, sputter-coated with gold, and mounted on aluminium holders specially designed for thin films. Secondary electron images were taken using in-lens detector at beam voltage value of 3 keV.

Transmission electron microscopy (TEM) was performed on a JEOL 1200 TEM on very thin (~70 nm) slice placed over 300-mesh copper grids cut using ultra microtome from 100–150 μm thick films of the hybrids. The acceleration voltage was 120 keV, and the magnification of the reported image is 120 kX.

The roughness, aerial topography and surface textures were measured using a ZYGO optical surface profilometer Model 6300 with scanning white-light interferometry (SWLI) as core technology.

Fourier transformed infrared (FTIR) spectra of the pristine PIs and their hybrids were recorded in the range of 400–4000 cm^{-1} using a Perkin-Elmer FTIR 2000 spectrometer to confirm the imidization reaction and to study the nature of the silica network formation. Thin films of around 10 μm thickness were used for spectroscopic analysis. the spectra obtained were normalized to remove errors due to uneven/non-uniform thickness of the films, using the ring-breathing mode of organic moieties at 1500 cm^{-1} as this band does not participate in the imidization process (21).

3 Results and Discussion

3.1 Morphology of the Hybrid Films

The FE-SEM micrographs of fractured surfaces of the hybrids utilizing PI without hydroxyl groups i.e., PIH-x with 10, 20 and 30 wt% silica, respectively are given in Figure 2(a1, b1, and c1). The dispersed silica particles are in the form of white beads having smooth surface with clear sharp boundaries showing no signs of interactions with the surrounding matrix. The average size of uniformly dispersed, silica particles increases from 1.2 μm to 5.0 μm as the silica content in the matrix increases from 10 to 30 wt%. Uniform dispersion of spherical particles suggests that it may be outcome of spinodal decomposition process that took place during drying and condensation at elevated temperature. Higher magnification images of a portion from a typical SEM image of PIH-x system, shown in Figure 3(a), clearly demonstrate these details. Phase separation is the result of thermodynamic immiscibility between organic and inorganic components. The gap of 0.1 to 0.5 μm between the particles and the matrix is created due to unequal shrinkage in the polymer matrix as a result of solvent evaporation, imidization process and the condensation reaction in the silica network during the sol-gel process.

The SEM micrographs of hybrids prepared with hydroxyl groups bearing PI i.e., PHIH-x, with 10, 20 and 30 wt% silica are shown, respectively, in Figure 2(a2, b2, and c2). These micrographs apparently show two different types of population of silica particles, one of 20–70 nm size and a second with a larger dimension i.e., 0.3–1.3 μm. However, a

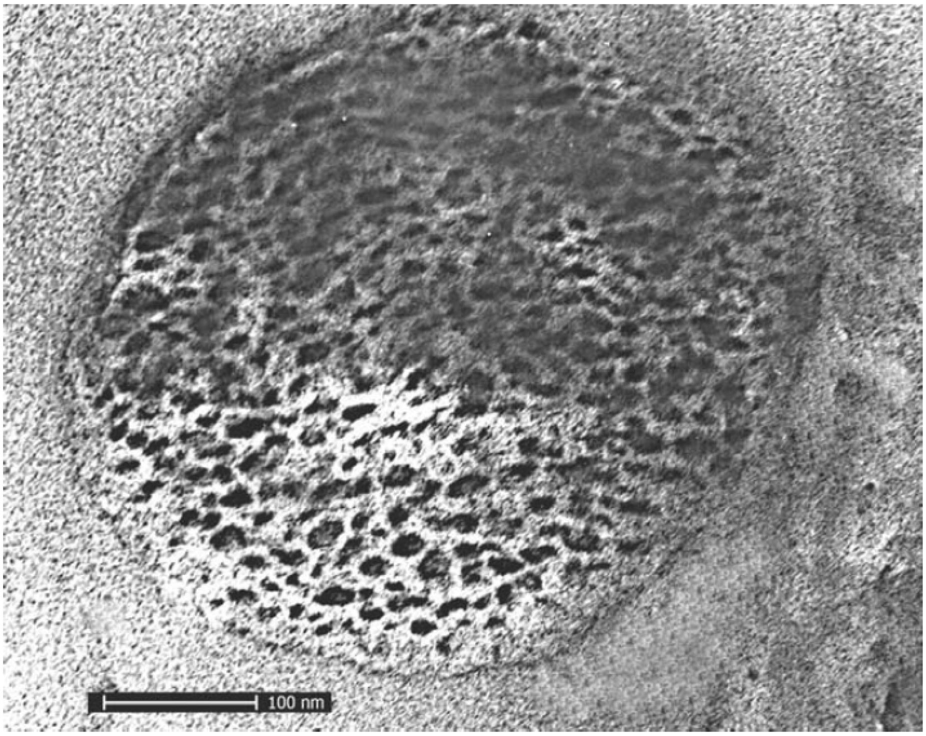

Fig. 4. TEM micrographs of a single particle of PHIH-10.

still magnified SEM image of a representative section from PHIH-x system, shown in Figure 3(b), clearly demonstrates a totally different morphology as compared to the particles in PIH-x (Figure 3a) hybrid systems. The appearance of rough and granular surface with remains of broken structures at the boundary motivated us to investigate the internal morphology and make-up of these particles. For this purpose, a thin slice of the PHIH-x hybrid containing such particles was obtained using microtomy for the TEM examination. TEM micrograph, shown in Figure 4, revealed that these particles are actually a porous silica network, embedded in the polymer matrix. Hence, the PHIH-x hybrids, on the basis of observed morphology, can be viewed as being composed of two distinct phases: (i) a silica lean phase (SLP), and (ii) a silica rich phase (SRP). In SLP, silica particles of 20–70 nm sizes are dispersed in the matrix with varying inter-particle distances of 80–200 nm as evident from Figure 3(c). The SRPs, on the other hand, are composed of network structure or closely knitted 5–30 nm sized particles, with almost size-equivalent inter-particle distances. Presence of diffused boundaries and absence of gap between the inorganic phase and polymer surrounding each particle in SRP, shows strong adhesion that may be due to chemical interaction of silica clusters with polymer layer through hydroxyl groups. The rough and granular appearance of this layer, evident from Figure 3(b), suggests that curing might have caused the breaking of matrix chains in such a way that leaves covalently bound polymer layer at the surface of SRP.

Based on the observed morphology and structure of PHIH-x system hybrids, influence of hydroxyl-bearing matrix on morphology may be considered as a sequential two-step process. We propose a model, namely "Retain and React" based on the two-step process, to explain observed morphology. During dispersion of TEOS solution in PAA, in the first step, the pendant hydroxyl groups may interact with hydrolyzed TEOS molecules through hydrogen bonding, and may *retain* few hydrolyzed TEOS molecules around each hydroxyl group. This nucleation process may lead to uniform distribution of hydrolyzed TEOS molecules throughout the matrix. During the condensation step, these hydrolyzed TEOS molecules form $\sim$ 5 nm size primary clusters that may condense (*react*) with pendant hydroxyl groups, present both on the PI chains and on the surface of another such cluster in the vicinity, producing covalently coupled structure. Aggregation of such polymer bound silica clusters may yield SRP. It is expected that until the onset of condensation reactions, the SLP and SRP may be indistinguishable. However, increasing degree of condensation at elevated temperature causes shrinkage in SRP and SLP in opposite direction. Growing inward pull due to shrinkage, on both sides, may cause the two domains to break from each other at boundary where gradient exists. The roughness of the surface and existence of chemical linkages between the two phases at the boundary supports the postulate that entrapped and bound polymer chains entering and leaving these agglomerates break at the weakest point.

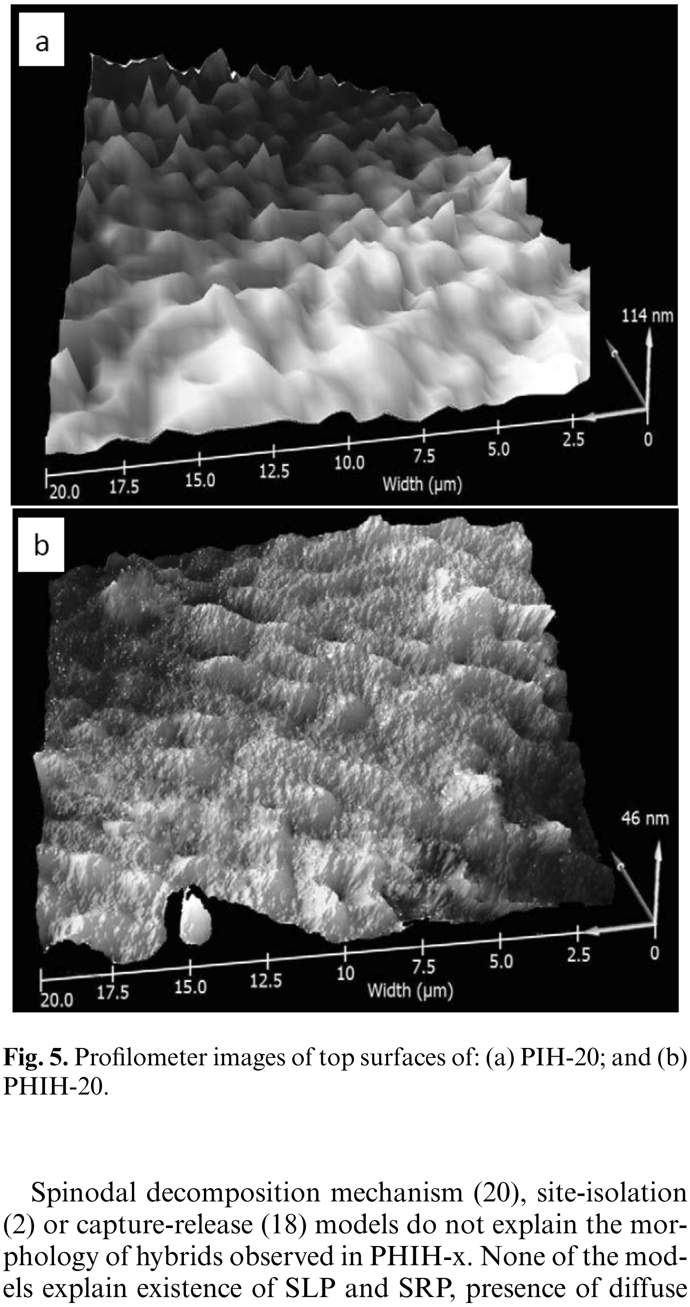

Fig. 5. Profilometer images of top surfaces of: (a) PIH-20; and (b) PHIH-20.

Spinodal decomposition mechanism (20), site-isolation (2) or capture-release (18) models do not explain the morphology of hybrids observed in PHIH-x. None of the models explain existence of SLP and SRP, presence of diffuse boundaries, and absence of gap between the particle and polymer as in PHIH-x system. Site-isolation and capture-release models may be used to explain formation and dispersion of two populations of particles, but existence of SLP and SRPs, where chemical interaction produces diffused boundaries that eliminate gap between the particle and polymer can only be explained if nucleation/retention is associated with hydrogen bonding and presence of diffused boundaries and chemical linkages with subsequent condensation reaction of pendant hydroxyl group on the chain with Si-OH. This co-continuous morphology, good adhesion, coupled with small particle size, can be attributed to the enhanced polarity of the matrix brought about by the hydroxyl groups present along the polymer chain.

3.2 Surface Profilometry

Surface roughness and texture were studied by a non-contact surface profilometer on the top of the specimens. Figure 5(a, b) shows profilometer images of the surfaces of PIH-20 and PHIH-20 systems respectively which are representative of their bulk composition/ morphology. Figure 5(a) shows almost equi-sized contours of 2–2.5 μm diameter with a roughness of 114 nm. Figure 5(b) shows bimodal distribution of contours on the surface with a roughness of 46 nm, representing a portion of embedded big and small silica particles lying near the top surface having 1–1.2 μm and 20–50 nm diameters respectively. These results compliment what SEM and TEM micrographs revealed about bulk of nano-composite systems, hence confirming important role of pendant hydroxyl groups in controlling the morphology and distribution of the inorganic component.

3.3 FTIR Studies

The process of imidization was measured through FTIR analysis. The spectra of the pristine PI, PHI and their hybrids with 10–30 wt% silica contents have been shown in Figure 6. The conversion of PAA to PI resulted in a disappearance of amide carbonyl peak at 1660 cm^{-1}and appearance of new absorption bands at 1777–1782, 1722–1730, and 1377–1380 cm^{-1} due to the asymmetric stretching of C=O, symmetric stretching of C=O and symmetric stretching of C-N respectively, which are assigned to the imide ring (22) thus confirming the complete curing of PAA to PI.

The nature of silica network produced in two types of hybrids has been analyzed and a detailed attempt been made to assign structural aspects to FTIR (Fig. 7) spectral features. Silica structures generated through sol-gel process using TEOS normally have three distinct absorptions centred respectively at 3000, 1090 and 460 cm^{-1}. The band at 3000 cm^{-1} corresponds to C-H stretching mode of residual alkyl groups, while the band at 1090 cm^{-1} is a complex profile with multiple contributions from various vibrational origins. Peak at 460 cm^{-1} is due to Si-O-Si bending mode absorption and its position depends upon equilibrium bond angles while its full width at half height (FWHH) is a sensitive measure of the distribution of Si-O-Si bond angles (23). In order to study the effect of enhanced chain polarity in case of PHIH-x and silica loading in both PIH-x and PHIH-x on the resulting silica structures, spectrum for each corresponding composition were plotted together and are being presented from three structurally important, regions:

3.4 Region 3800–2800 cm^{-1}

The absorption band centred around 3490 cm^{-1} in Figure 7(a) represents C-OH bond stretching and confirms the presence of hydroxyl group on the main chain in the case of pristine PHI, while this absorption peak is absent in pristine PI. It is evident from Figure 7(b-d) that broad

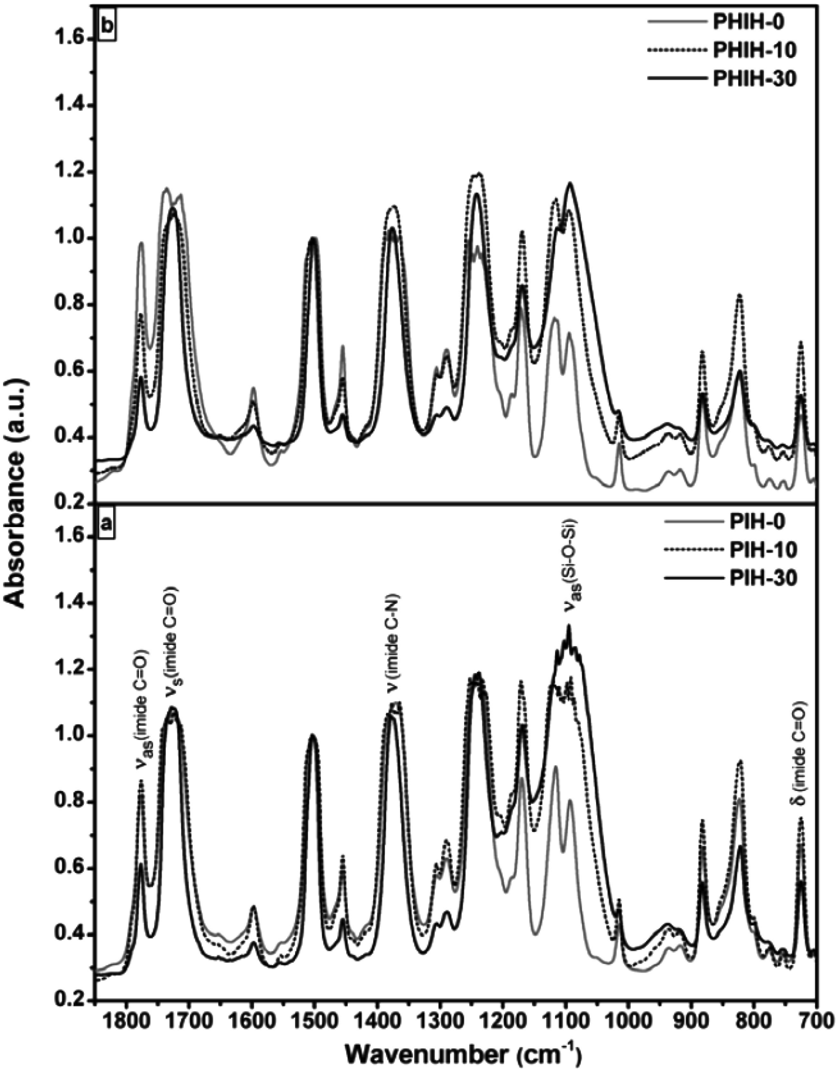

Fig. 6. FTIR spectra of polyimide/silica hybrids.

band 3700-3200 cm^{-1} centered around 3490 cm^{-1} broadens and increases in height as silica contents increases in the PHIH-x system. This may be due to the combined effect of C-OH bond stretching and uncondensed silanols (Si-OH) generated as a result of hydrolysis of TEOS. Higher absorption for this band in the case of PHIH-x as compared to PIH-x for same value of 'x' may be due to a higher number of uncondensed silanols that points toward the existence of diffused silica structures having collectively higher number of uncondensed silanols at their surfaces. Our SEM and TEM studies also confirmed the existence of nano-sized silica structures in PHIH systems (Figs. 2-4).

3.5 Region 1200-1000 cm^{-1}

The absorption band at 1150-1020 cm^{-1} is a complex profile with multiple contributions from different vibrational origins. Figure 7(f-h) shows a broad band around 1150-1020 cm^{-1} in both PIH-x and PHIH-x, whose width and height increases with increasing silica content from 10 to 30 wt%, confirms contribution of asymmetric stretching mode absorption of the Si-O-Si group that appears as doublet at 1091–1044 cm^{-1} and hence, confirms formation of three-dimensional Si-O-Si networks. This doublet is of particular interest as it carries distinct information on molecular structure of the silica network. To retrieve this information, difference spectra for both PIH-x and PHIH-x were obtained by subtracting respective pristine PI spectra from the spectra of PIH-x and PHIH-x. The ratio of absorbance of high wave number to low wave number components, shown in Figure 8, corresponds to cyclic and linear structures respectively, was calculated using difference spectra. It is evident that the ratio decreases significantly with increase in silica content for PHIH-x while negligible effect can be observed in PIH-x system. Decrease in absorbance ratio in case of PHIH-x indicates that amount of linear

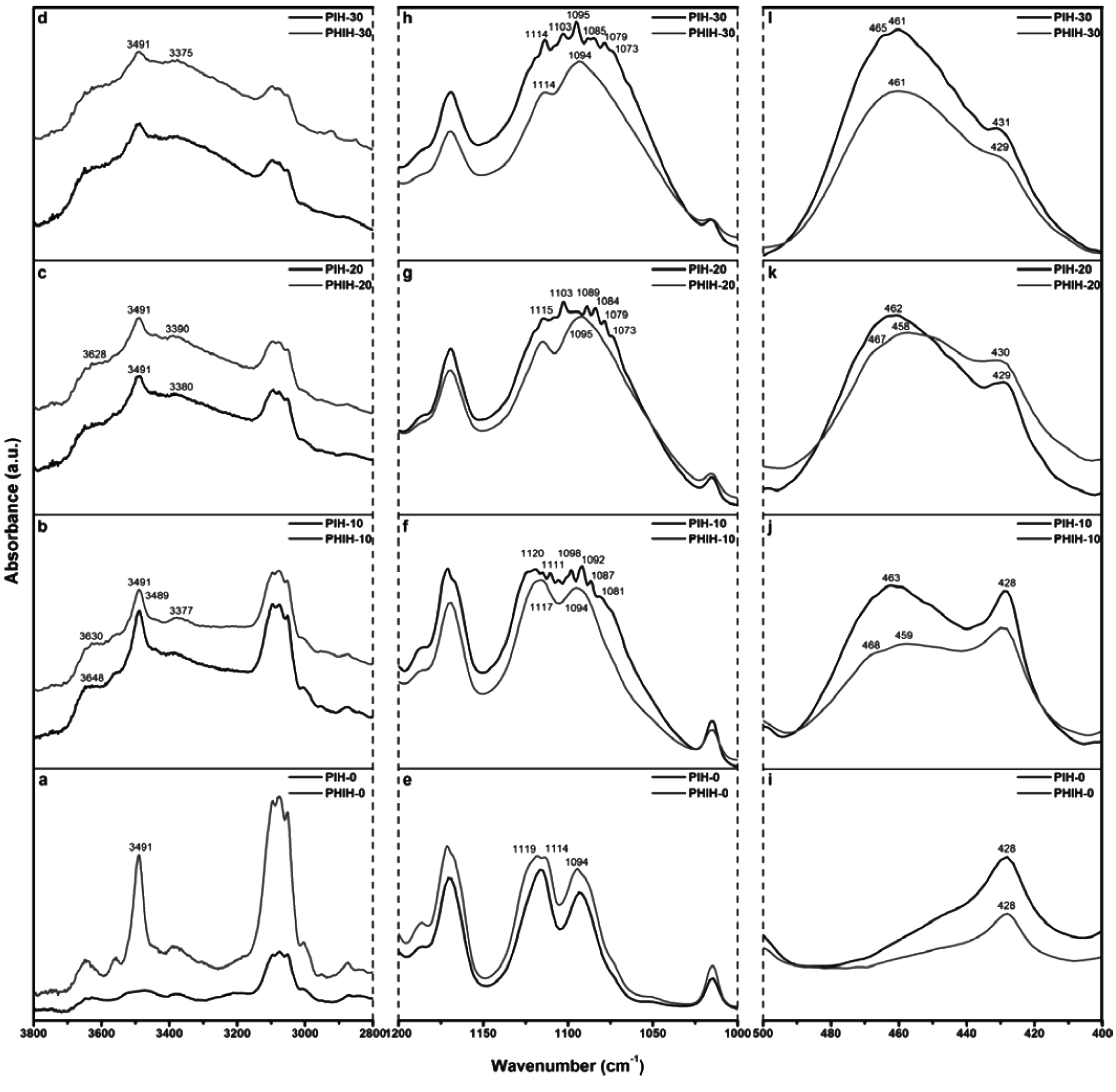

Fig. 7. FTIR spectra of polyimide/silica hybrids Absorbance scale: Graphs (a-d) 0.2–0.4, Graphs (e-f) 0.2–1.4, Graphs (i-1) 0.2–0.8.

structure is increasing as compared to cyclic structure. This phenomenon, where network connectivity decreases, points toward the behaviour of an organically modified structure as reported earlier (23).

It is important to note from Fig. 7(f–h) that in PHIH-x, the width of the band for corresponding silica loading is much less as compared to their counterparts in PIH-x, indicating a narrow distribution of closely resembling silica clusters in PHIH-x, while the broad band may be due to the dissimilar nature of clusters.

It can also be observed that the height of the bands for PIH-x is more as compared to PHIH-x. The dense cyclic structures having a high number of Si-O-Si bonds are expected to absorb more during asymmetric stretching as compared to linear structures. Hence, it can be concluded that PIH-x has condensed/cyclic structure while PHIH-x have an open structure.

Surface Si-OH groups may interact with matrix material and with other similar inorganic structures in their vicinity. Interaction with matrix through covalent bonds yield

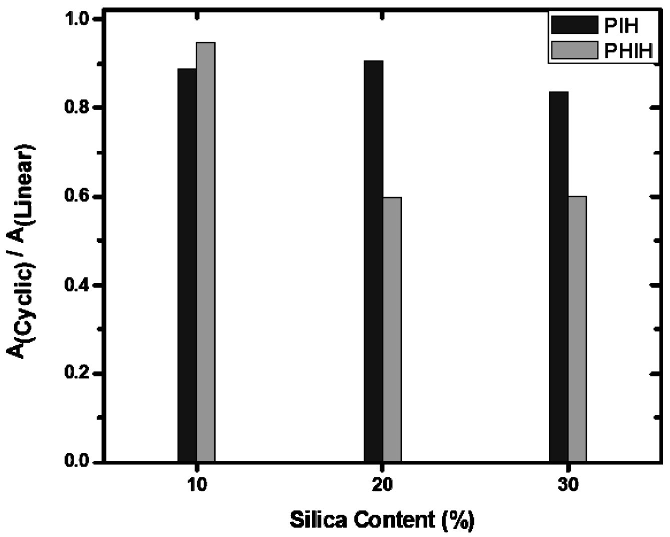

Fig. 8. Ratio of A(Cyclic)/A(Linear) for PIH-x and PHIH-x based on difference spectra of Si-O-Si asymmetric stretching mode absorption.

structures similar to organically modified co-continuous structures. Asymmetric stretching mode of Si-O-C contributes to the complex absorption band at 1150–1020 cm^{-1}(23). Hence, the coupling between the inorganic and organic domains is established through Si-O-C link, resulting in reduced silica particles size with diffused boundaries.

3.6 Region 500–400 cm^{-1}

Bending mode of the Si-O-Si bonds give rise to the absorption band centred around 463 cm^{-1} as shown in Figure 7(j-l). Broadening of the band is associated with structural irregularity as found in the modified silica networks (23). Spectral subtraction was performed to eliminate contribution of PI and Full Width at Half Height (FWHH) values were calculated using these difference spectra. Figure 9 shows the representative difference spectra. Higher FWHH values for PHIH-x as compared to PIH-x systems (Fig. 10) show broader distribution of Si-O-Si bond angles for PHIH-x systems and hence, reflect reduction in structural regularity and interconnectivity. It can be inferred that reaction of -Si-OH with pendant hydroxyl group resulted in a modified silica network structure showing influence of pendant hydroxyl groups on the morphology. Peak position is another indicator that supports the effect of pendant hydroxyl groups on the morphology. It has been reported in the case of pure silica derived from pure TEOS system, the peak occurs at 463 cm^{-1} while in the organically modified TEOS system, its maxima occurs at 456 cm^{-1}(24)/. In our case, PHIH-x peaks appear at lower wave numbers, indicating organically modified silica behaviour with structural irregularity and hence bigger bond angles. The peak, in the case of PIH-x, appears at higher wave numbers, representing pure silica behaviour with structural regularity and hence smaller bond angles. It can be concluded that morphology and silica network structure can thus be modified by incorporating hydroxyl groups in the matrix polymer.

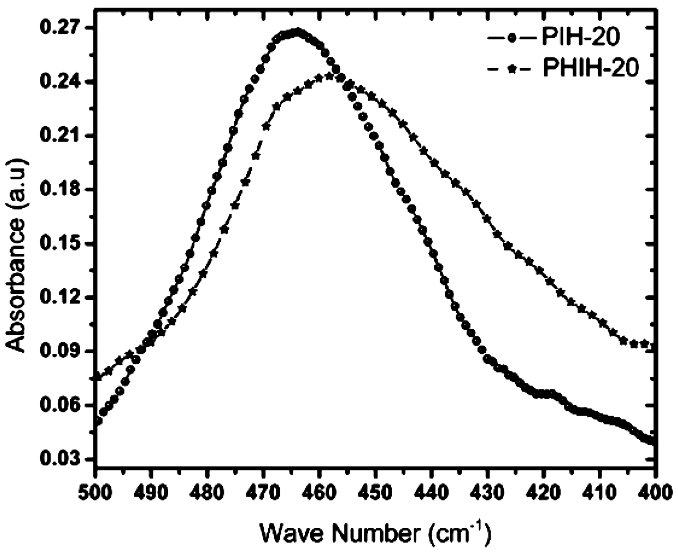

Fig. 9. Difference spectra of PIH-20 and PHIH-20.

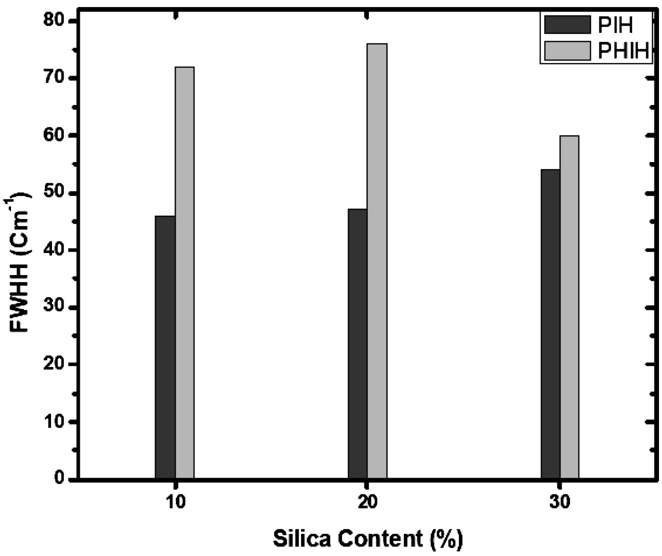

Fig. 10. FWHH data of Si-O-Si bending mode of absorption vs. Silica contents for PIH-x and PHIH-x.

4 Conclusions

The presence of hydroxyl groups on polyimide backbone plays an important role in dictating the morphology of the resulting PI-silica hybrids. Silica clusters composed of co-continuous nano-domains are formed in hydroxyl-bearing matrix as compared to condensed micron-sized silica particles with smooth surfaces in case of PI chain without such groups. A model namely "Retain and React" based on a two-step process, has been proposed to explain the observed morphology as the spinodal decomposition mechanism, site-isolation or capture-release models can not explain satisfactorily the existence of SLP and SRP, diffuse boundaries, and absence of gap between the particle and polymer in such hybrid systems.

References

1. Ghosh, M.K. and Mittal, K.L. *Polyimides: Fundamentals and Applications*. Marcel Dekker: New York, 1996.
2. Nandi, M., Conklin, J.A., Salvati, L. and Sen, A. (1991) *Chem. Mater.,* 3(1), 201–206.
3. Morikawa, A., Iyoku, Y., Kakimoto, M. and Imai, Y. (1992) *Polym. J,* 24(1), 107–113.
4. Morikawa, A., Yamaguchi, H., Kakimoto, M. and Imai, Y. (1994) *Chem. Mater.,* 6(7), 913–917.
5. Mascia, L. and Kioul, A. (1994) *J Mater. Sci. Lett.,* 13(9), 641–643.
6. Morikawa, A., Iyoku, Y., Kakimoto, M. and Imai, Y. (1992) *J Mater. Chem.,* 2(7), 679–690.
7. Wang, S.H., Ahmad, Z. and Mark, J.E. (1994) *Chem. Mater.,* 6(7), 943–946.
8. Kioul, A. and Mascia, L. (1994) *J Non-Crystall. Solids,* 175(2–3), 169–186.
9. Mascia, L. and Kioul, A. (1995) *Polym.,* 36(19), 3649–3659.
10. Al-Kandary, S., Ali, A.A.M. and Ahmad, Z. (2006) *J. Mater. Sci.,* 41(10), 2907–2914.
11. Al-Kandary, S., Aliand, A.A.M. and Ahmad, Z. (2007) *J. Adv. Mater.,* 105–113.
12. Khalil, M., Saeed, S. and Ahmad, Z., (2008) *J. Appl. Polym. Sci.,* 107(2), 1257–1268.
13. Chen, B-K., Chiu, T.-M. and Tsay, S-Y. (2004) *J. Appl. Polym. Sci.,* 94(1), 382–393.
14. Rehman, H.U., Schmidt, H. and Ahmad, Z. (2006) *J. Macromol. Sci., Part A-Pure and Appl. Chem.,* 43(4–5), 703–717.
15. Ahmad, Z., Aliand, A.A.M., AlSagheer, F. and Al-Arbash, A., (2006) *Inter. J. Polym. Mater.,* 55, 103–120.
16. Huang, Y. and Gu, Y., (2003) *J. Appl. Polym. Sci.,* 88(9), 2210–2214.
17. Huang, Y., Qin, J.Q. and Gu, Y. (2004) *J. Appl. Polym. Sci.,* 93(3), 1198–1202.
18. Qin, J.Q., Zhao, H., Liu, X.Y., Zhang, X.Y. and Gu, Y. (2007) *Polym.,* 48(12), 3379–3383.
19. Joly, C., Smaihi, M., Porcar, L. and Noble, R.D. (1999) *Chem. Mater.,* 11(9), 2331–2338.
20. Inoue, T. (1995) *Progress in Polymer Science,* 20(1), 119–153.
21. Khalil, M., Saeed, S. and Ahmad, Z. (2007) *J Macromol. Sci., Part A-Pure and Appl. Chem.,* 44(1), 55–63.
22. Yang, C.P. and Lin, J.H. (1994) *J. Polym. Sci., Part A: Polym. Chem.,* 32(2), 369–382.
23. Musto, P., Abbate, M., Lavorgna, M., Ragosta, G. and Scarinzi, G. (2006) *Polym.,* 47(17), 6172–6186.
24. Mauritz, K.A. and Warren, R.M. (1989) *Macromol*, 22, 1730–1734.